

## Supporting information

### A sensitive fluorescent sensor based on terpyridine@Zn<sup>2+</sup> modified mesoporous silica for the detection of sulfonamide antibiotics

Qian Zhao and Jing Wang\*

School of Chemistry and Chemical Engineering, Guangxi University, Nanning 530004, PR China

Corresponding author, e-mail: [wjwyj82@gxu.edu.cn](mailto:wjwyj82@gxu.edu.cn)

**Table S1** BET surface area ( $S_{\text{BET}}$ ), Total pore volume ( $V_{\text{total}}$ ) and average pore diameters ( $D_{\text{BJH}}$ ) for ATpy@Zn-SBA-15 calculated from the N<sub>2</sub> adsorption-desorption isotherms

| Sample                 | $S_{\text{BET}}$ (m <sup>2</sup> /g) | $V_{\text{total}}$ (cm <sup>3</sup> /g) | $D_{\text{BJH}}$ (Å) |
|------------------------|--------------------------------------|---|----------------------|
| SBA-15 <sup>[S1]</sup> | 486                                  | 1.24                                    | 102.0                |
| ATpy@Zn-SBA-15         | 332                                  | 0.96                                    | 110.5                |

**Table S2** The fluorescence decay parameters of ATpy@Zn-SBA-15 in the absence and presence of STZ and SMT

| Samples            | $T_1$ (ns) | $B_1$  | $T_2$ (ns) | $B_2$  | $\tau$ (ns) |
|--------------------|------------|--------|------------|--------|-------------|
| ATpy@Zn-SBA-15     | 1.97       | 0.2062 | 25.41      | 0.0020 | 2.20        |
| ATpy@Zn-SBA-15@STZ | 2.57       | 0.1582 | 127.21     | 0.0024 | 4.47        |
| ATpy@Zn-SBA-15@SMT | 2.41       | 0.1713 | 123.26     | 0.0028 | 4.32        |

**Table S3** Energy of HOMO and LUMO of ATpy@Zn-SBA-15 and SAs

|           | ATpy@Zn <sup>2+</sup> | STZ       | SMT      | SCP        | SMR        | SMP      |
|-----------|-----------------------|-----------|----------|------------|------------|----------|
| pKa       |                       | 2.0; 7.24 | 2.1; 5.3 | 1.87; 5.45 | 2.22; 6.80 | 2.2; 7.2 |
| HOMO (eV) | -2.68                 | -5.99     | -6.49    | -6.29      | -6.25      | -6.08    |
| LUMO (eV) | -1.51                 | -1.77     | -2.34    | -1.76      | -1.21      | -1.45    |
| Eg (eV)   | 1.17                  | 4.21      | 4.15     | 4.53       | 5.04       | 4.63     |

**Table S4** Comparison of the sensing and adsorption performance for different sulfonamide antibiotics from water by different materials

| Materials      | Methods      | SAs      | LOD                        | pH range | Application                     | Refs.     |
|----------------|--------------|----------|----------------------------|----------|---------------------------------|-----------|
| ATpy@Zn-SBA-15 | Fluorescence | STZ      | 0.17 $\mu\text{M}$         | 2.0-13.0 | Tap water and milk              | This work |
|                |              | SMT      | 0.63 $\mu\text{M}$         |          |                                 |           |
|                |              | SCP      | 0.52 $\mu\text{M}$         |          |                                 |           |
|                |              | SMR      | 0.57 $\mu\text{M}$         |          |                                 |           |
|                |              | SMP      | 0.54 $\mu\text{M}$         |          |                                 |           |
| N, B, F-CDs    | Fluorescence | STZ      | 5.5 ng L <sup>-1</sup>     | 3.0-10.0 | Soil, river water, milk and egg | [S2]      |
| FCS-1          | Fluorescence | SCP      | NA                         | 3.0-9.0  | NA                              | [S3]      |
| Cu NCs         | Fluorescence | STZ      | 0.23 $\mu\text{g mL}^{-1}$ | 8.5      | Honey and milk                  | [S4]      |
| Microspheres   | HPLC         | SMR      | NA                         | 5.0      | Milk and egg                    | [S5]      |
| MIPs           | HPLC         | STZ, etc | 0.013 $\mu\text{g L}^{-1}$ | 7.0      | Lake water and well water       | [S6]      |
| PAN/Tp-BD      | HPLC         | SCP      | 0.18 ng L <sup>-1</sup>    | 4.0      | Chicken and fish                | [S7]      |
|                |              | SMP      | 0.10 ng L <sup>-1</sup>    |          |                                 |           |

LOD: Limit of detection; NA: Not available; NCs: Nanoclusters

## References

- [S1]. Huang J, Wang J, Li D, Chen P, Liu HB (2021) Terthiophene-functionalized mesoporous silica-based fluorescence sensor for the detection of trace methyl orange in aqueous media. *Mikrochim Acta* 188: 410.
- [S2]. Chen L, Liu Y, Cheng G, Fan Z, Yuan J, He S, Zhu G (2021) A novel fluorescent probe based on N, B, F co-doped carbon dots for highly selective and sensitive determination of sulfathiazole. *Sci Total Environ* 759: 143432.
- [S3]. Zhu XD, Zhang K, Wang Y, Long WW, Sa RJ, Liu TF, Lu J (2018) Fluorescent Metal–Organic Framework (MOF) as a highly sensitive and quickly responsive chemical sensor for the detection of antibiotics in simulated wastewater. *Inorg Chem* 57: 1060–1065.
- [S4]. Sadeghi S, Oliaei S (2021) Microextraction of sulfathiazole from milk and honey samples using a polymeric ionic liquid membrane followed by fluorometric determination. *J Food Compos and Anal* 97: 103774.
- [S5]. Kilic G, Osman B, Tuzmen N (2018) Application of affinity microspheres for effective SPE cleanup before the determination of sulfamerazine by HPLC. *Mater Sci Eng C Mater Biol Appl* 91: 55–63.
- [S6]. Fan Y, Zeng G, Ma X (2020) Effects of prepolymerization on surface molecularly imprinted polymer for rapid separation and analysis of sulfonamides in water. *J Colloid Interface Sci* 571: 21–29.
- [S7]. Chen A, Guo H, Luan J, Li Y, He X, Chen L, Zhang Y (2022) The electrospun polyacrylonitrile/covalent organic framework nanofibers for efficient enrichment of trace sulfonamides residues in food samples. *J Chromatogr A* 1668:462917

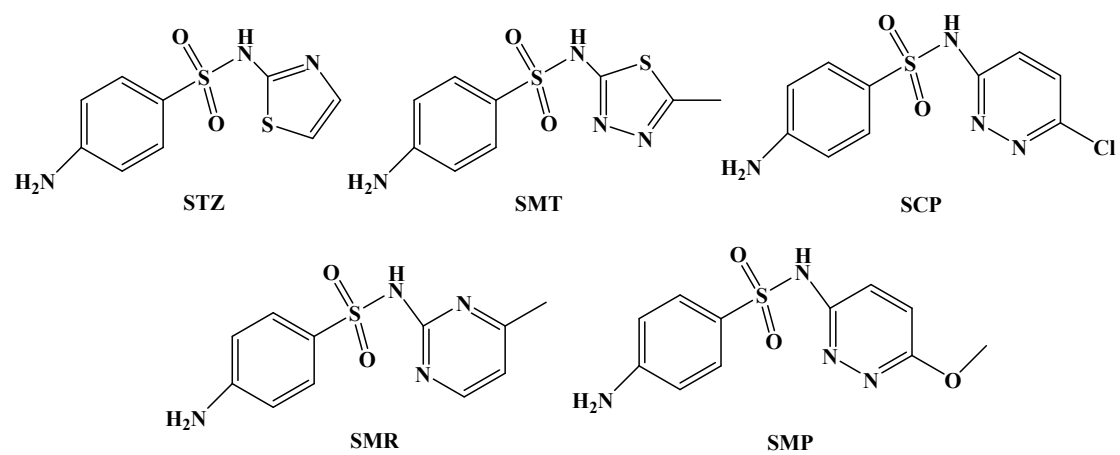


**Fig. S1** Molecular structures of SAs

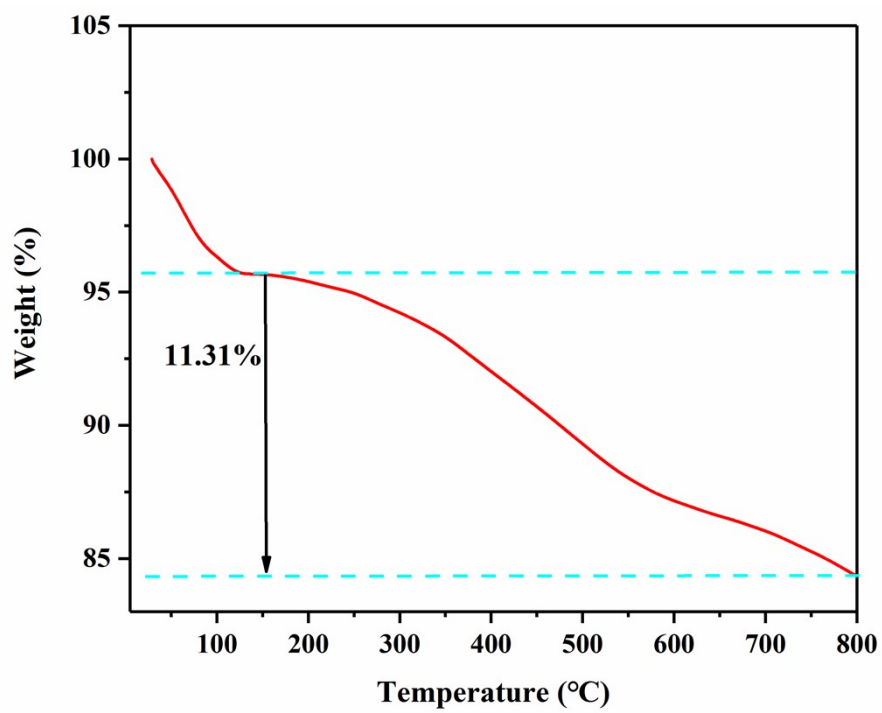


**Fig. S2** The TGA curve of ATpy@Zn-SBA-15

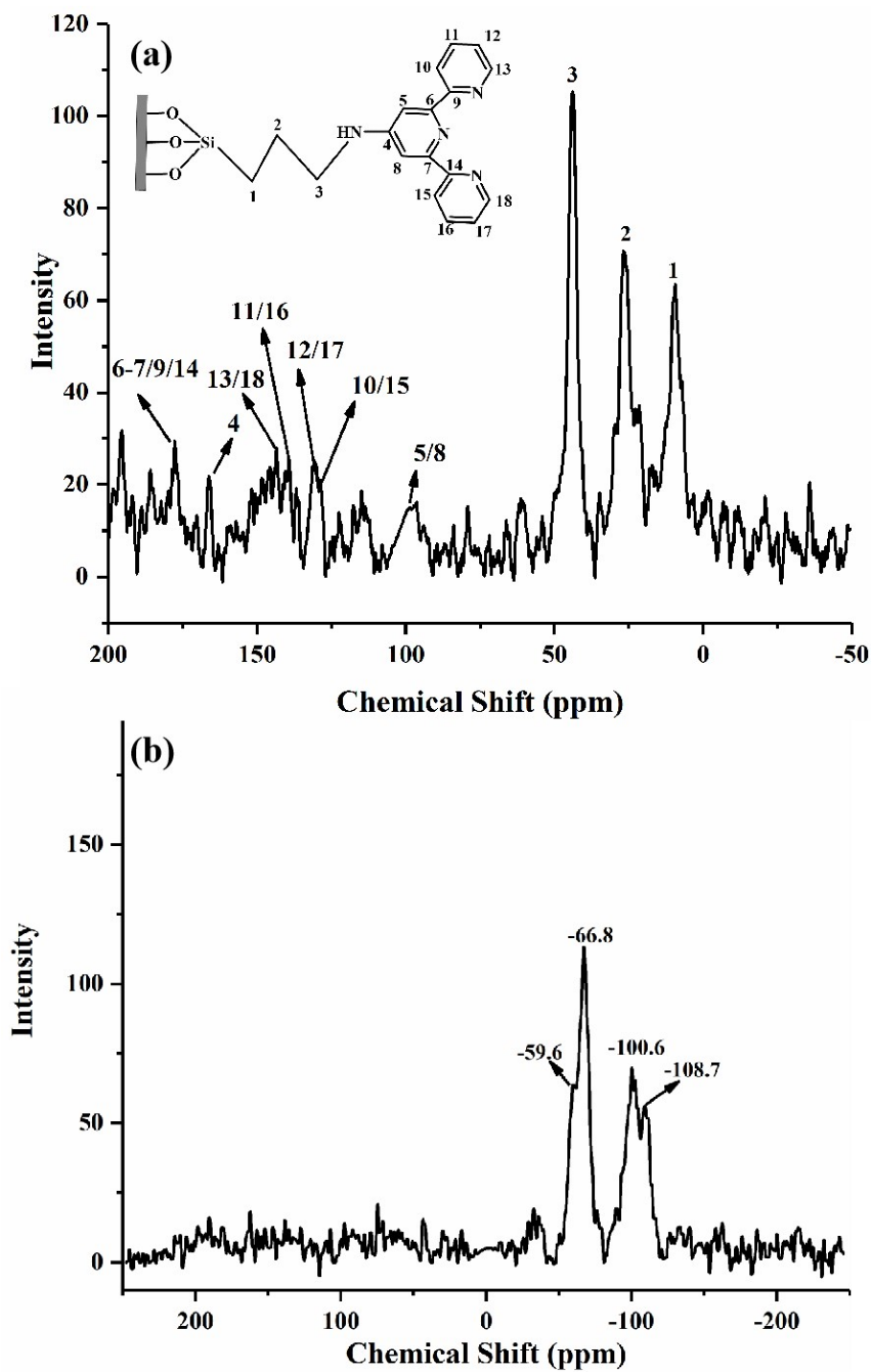


**Fig. S3** (a)  $^{13}\text{C}$  CP MAS NMR and (b)  $^{29}\text{Si}$  CP MAS NMR spectra of CTY@SBA.

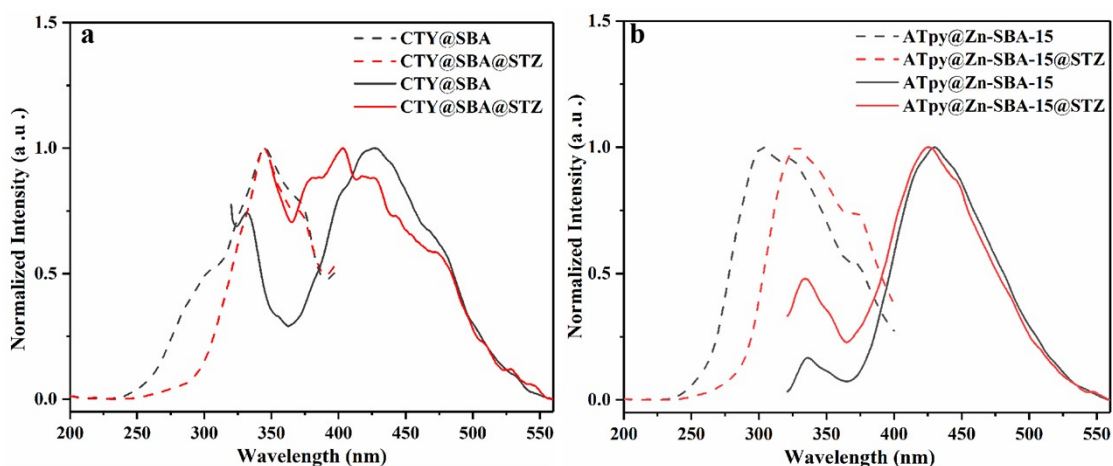


**Fig. S4** The normalized excitation and emission spectra of (a) **CTY@SBA** ( $0.05 \text{ g L}^{-1}$ ) and **CTY@SBA@STZ** ( $0.05 \text{ g L}^{-1}$ – $2.0 \times 10^{-4} \text{ M}$ ); (b) **ATpy@Zn-SBA-15** ( $0.05 \text{ g L}^{-1}$ ) and **ATpy@Zn-SBA-15@STZ** ( $0.05 \text{ g L}^{-1}$ – $2.0 \times 10^{-4} \text{ M}$ ) in aqueous solution (20 mM HEPES buffer, pH = 7.0)

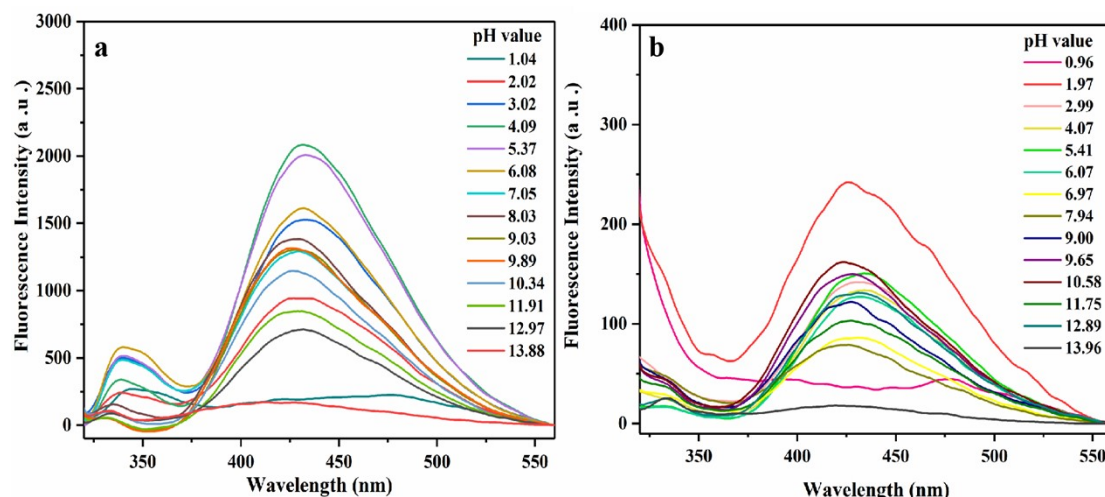


**Fig. S5** Fluorescence spectra of **ATpy@Zn-SBA-15** ( $0.05 \text{ g/L}$ ) in the absence (a) and presence (b) of **STZ** ( $2.0 \times 10^{-4} \text{ M}$ ) at different pH values.

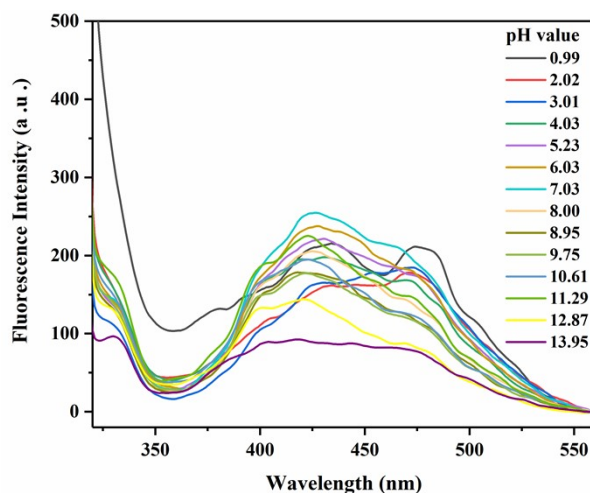


**Fig. S6** Fluorescence spectra of **CTY@SBA** ( $0.05 \text{ g/L}$ ) at different pH values.

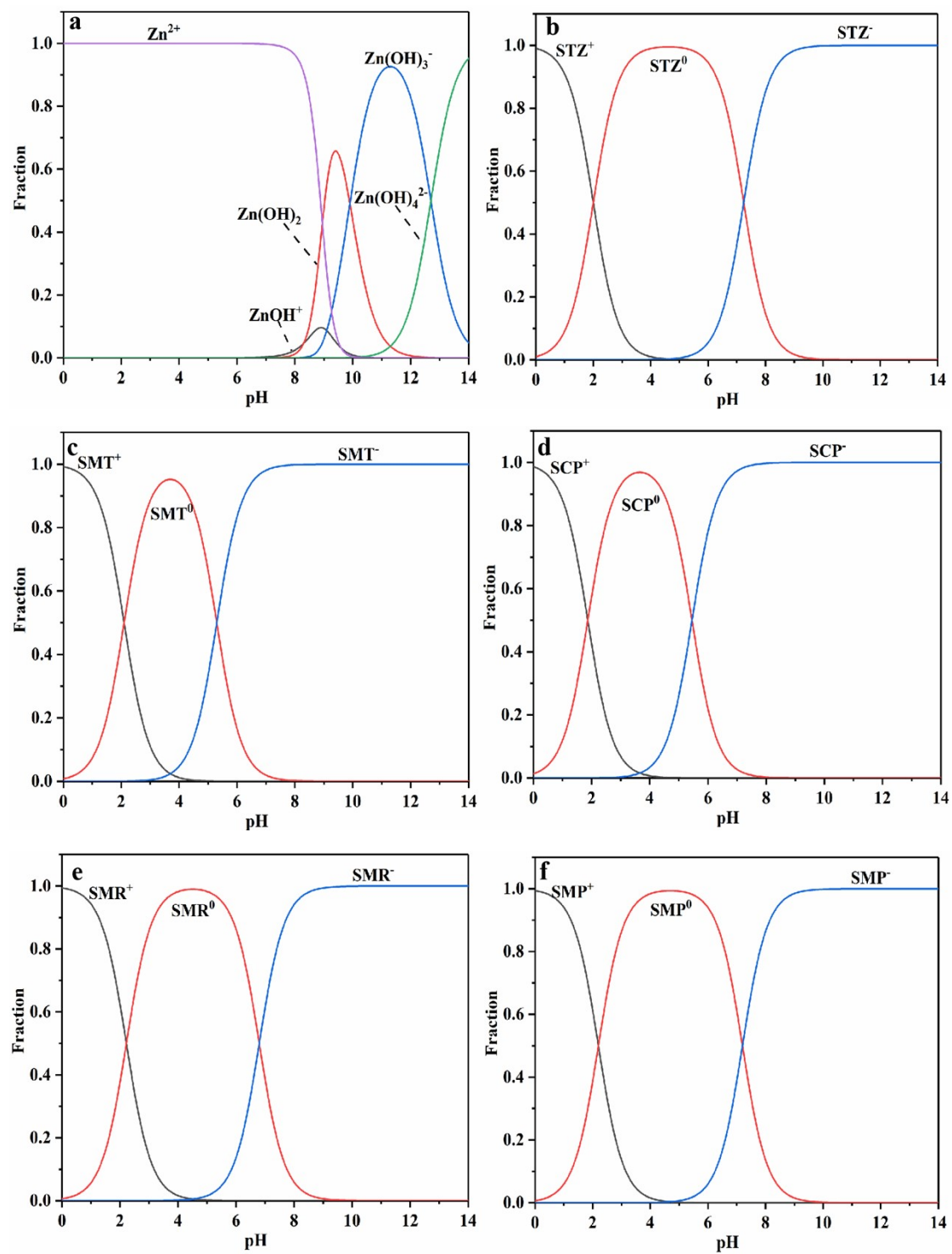


**Fig. S7** Distribution coefficient plot of Zn (a), STZ (b), SMT (c), SCP (d), SMR (e) and SMP (f) as a function of solution pH.

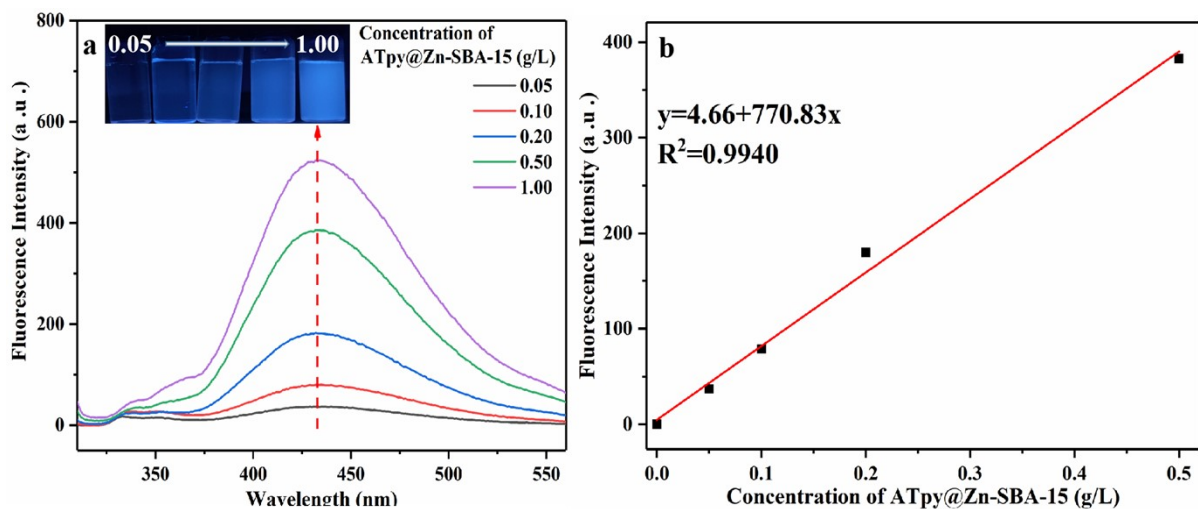


**Fig. S8** (a) The fluorescence spectra of ATpy@Zn-SBA-15 (0.05–1.00 g/L) in aqueous solution (20 mM HEPES buffer, pH = 7.0) ( $\lambda_{\text{ex}} = 298$  nm; slit: 3/5 nm); Inset: fluorescence images of different concentrations of ATpy@Zn-SBA-15 under 365 nm UV irradiation; (b) fluorescence intensity at 429 nm versus the concentration of ATpy@Zn-SBA-15

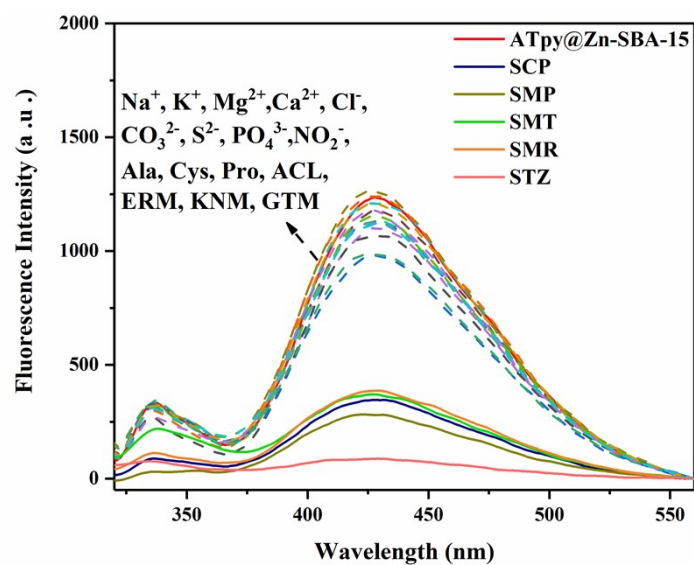


**Fig. S9** Fluorescence emission spectra of ATpy@Zn-SBA-15 (0.05 g/L) in the presence of various metal cations, anions, amino acid and antibiotics ( $2.0 \times 10^{-4}$  M) (20 mM HEPES buffer, pH = 7.0).



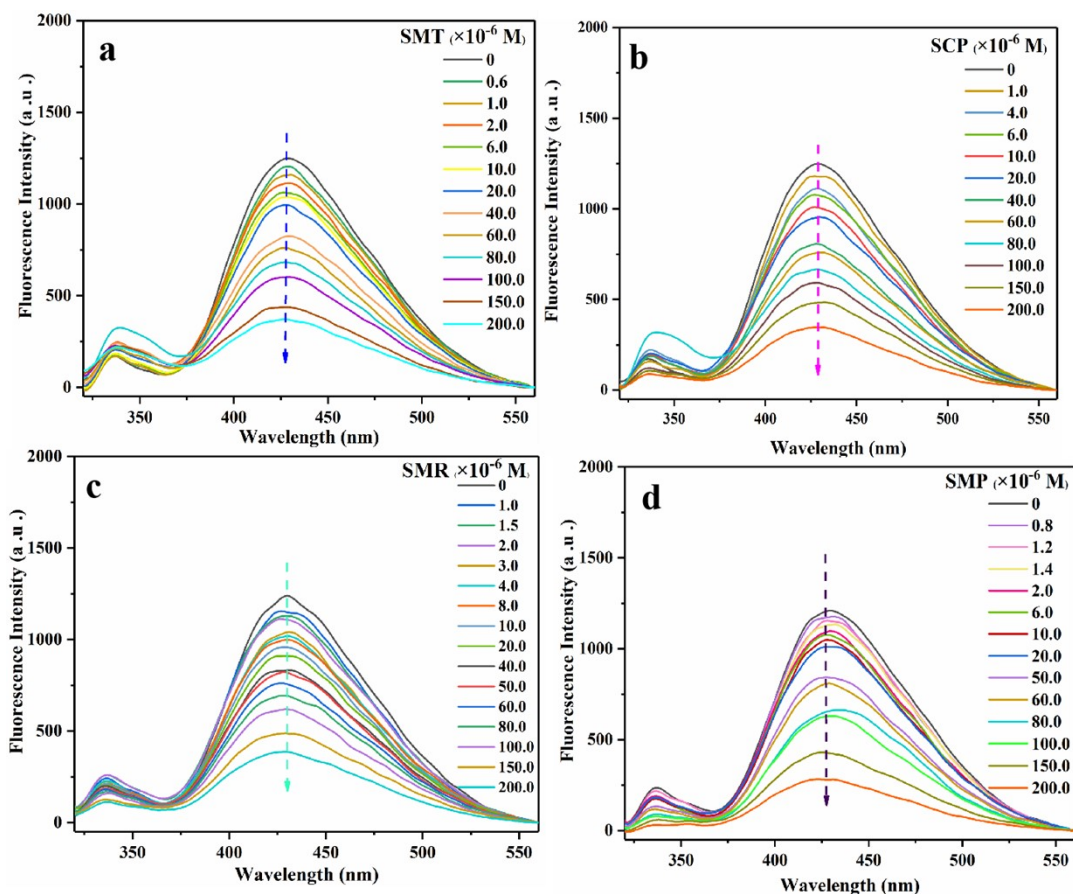


**Fig. S10** The fluorescence spectra of ATpy@Zn-SBA-15 (0.05 g/L) in the presence of different concentrations of (a) SMT ( $0-2.0 \times 10^{-4}$  M), (b) SCP ( $0-2.0 \times 10^{-4}$  M), (c) SMR ( $0-2.0 \times 10^{-4}$  M) and (d) SMP ( $0-2.0 \times 10^{-4}$  M) (20 mM HEPES buffer, pH = 7.0).

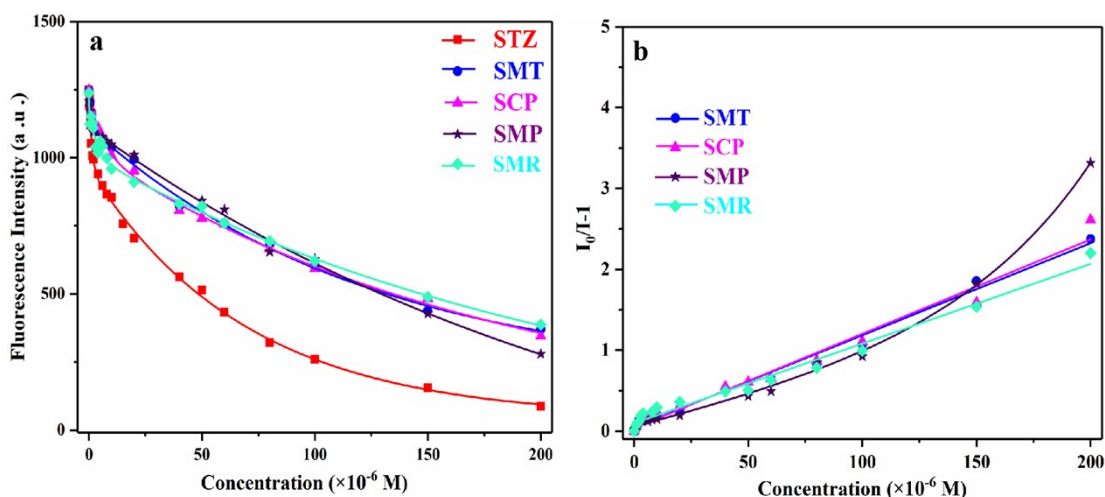


**Fig. S11** (a) The fluorescence intensity of ATpy@Zn-SBA-15 ( $0.05 \text{ g L}^{-1}$ ) and (b) the Stern-Volmer curve towards SAs at 429 nm in aqueous solution (20 mM HEPES buffer, pH = 7.0)

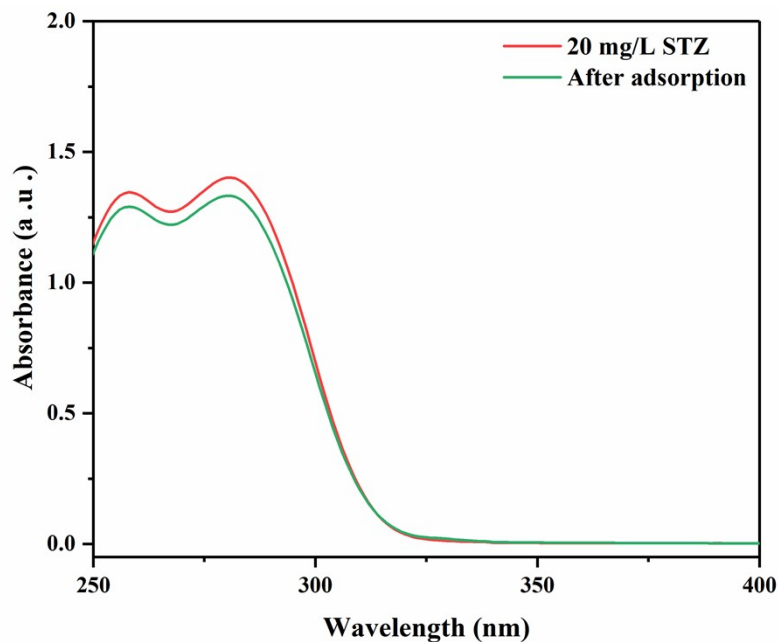


**Fig. S12** UV-Vis spectra for the adsorption of ATpy@Zn-SBA-15 toward STZ ( $W=5$  mg;  $V=10$  mL;  $C_0=20$  mg/L) after 6 h.

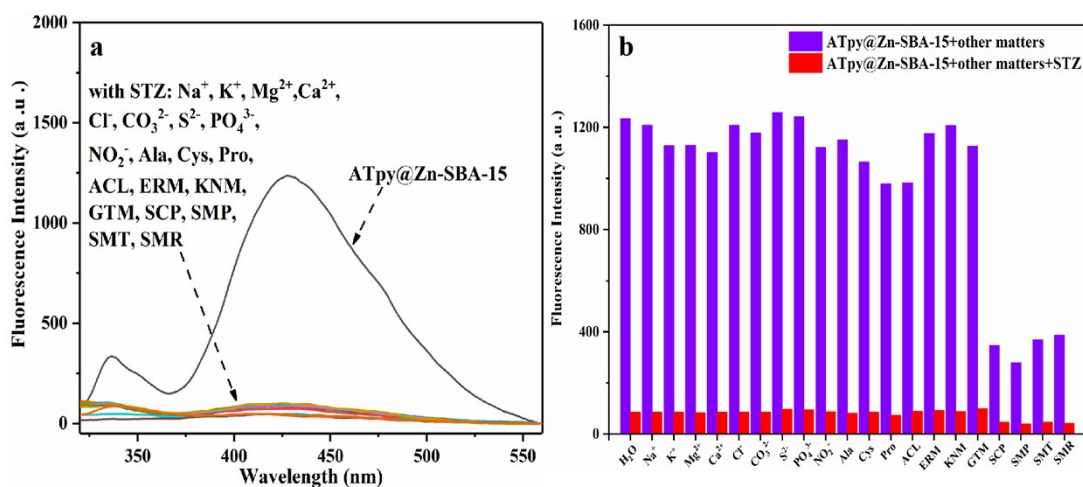


**Fig. S13 (a)** Fluorescence spectra and (b) the comparison of fluorescence intensity of ATpy@Zn-SBA-15@STZ ( $0.05$  g/L –  $2.0 \times 10^{-4}$  M) in the presence of metal ions, anions, amino acid and other antibiotics ( $2.0 \times 10^{-4}$  M) at HEPES buffer (20 mM, pH=7.0)

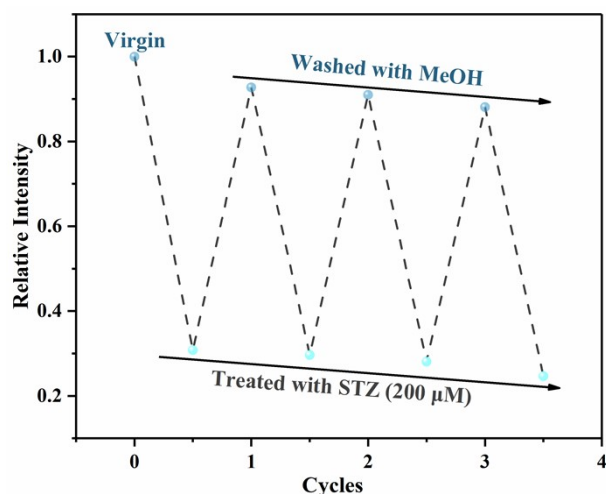


**Fig. S14** Recycling performance of ATpy@Zn-SBA-15 aqueous suspension ( $1.0 \text{ g L}^{-1}$ ) for the fluorescence detection of STZ aqueous solution ( $200 \text{ }\mu\text{M}$ ) when excited at  $298 \text{ nm}$ .

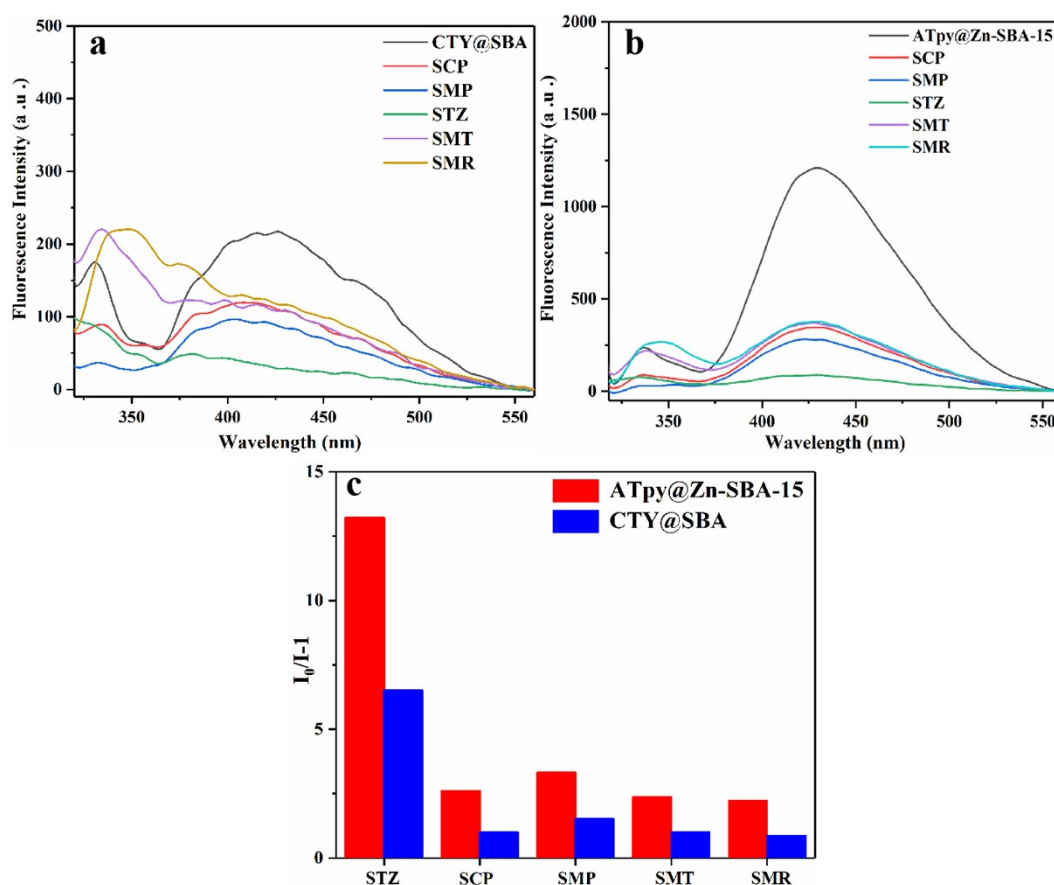


**Fig. S15** (a) Fluorescence spectra of CTY@SBA ( $0.05 \text{ g/L}$ ) and (b) ATpy@Zn-SBA-15 ( $0.05 \text{ g/L}$ ) in the presence of SAs ( $2.0 \times 10^{-4} \text{ M}$ ) in HEPES buffer ( $20 \text{ mM}$ ,  $\text{pH}=7.0$ ); (c) response of CTY@SBA and ATpy@Zn-SBA-15 toward SAs ( $I_0$  and  $I$  represent the fluorescence intensity at  $429 \text{ nm}$  in the absence and presence of each of SAs)

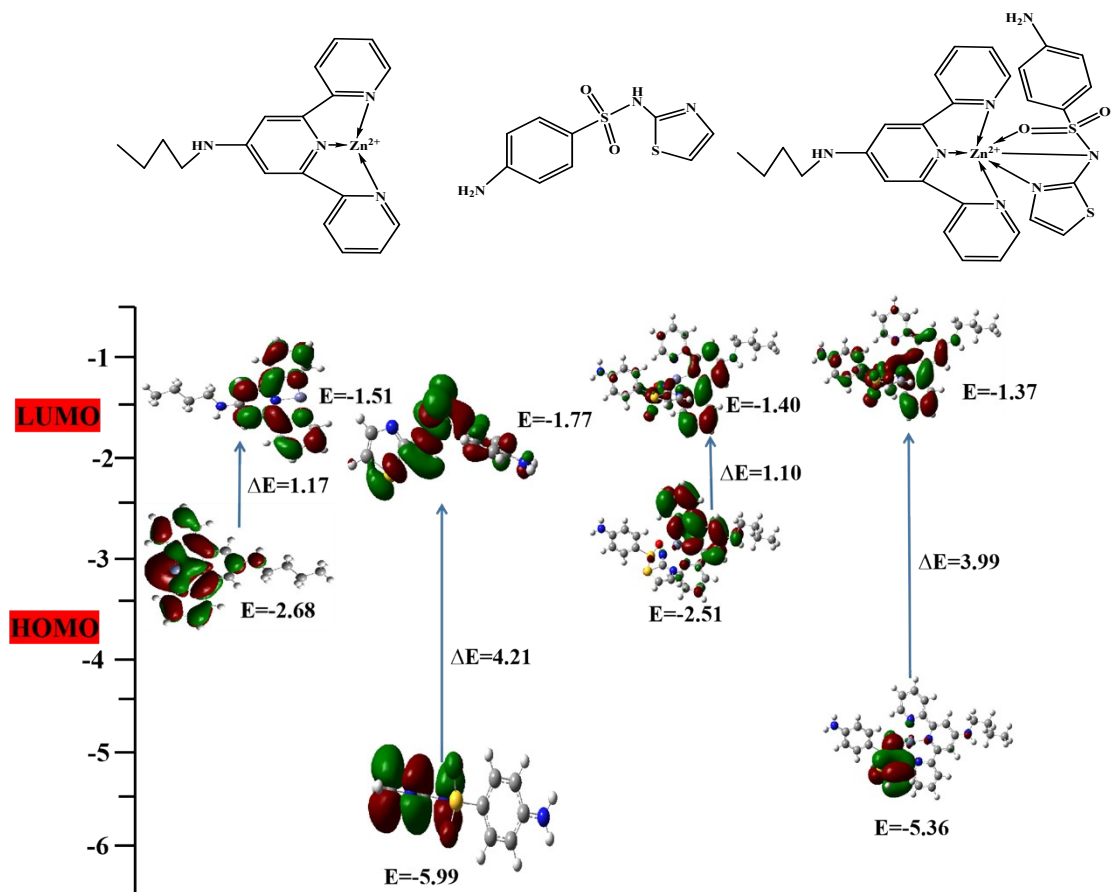


**Fig. S16** Theoretical HOMO and LUMO energies for ATpy@Zn-SBA-15, STZ and ATpy@Zn-SBA-15@STZ